

# High Hardness and Anti-Reflective Films for Displays Application

**Nizamidin Jappar** [www.kimototech.com](http://www.kimototech.com)

Presented at the 20<sup>th</sup> International Coating Science and Technology Symposium  
September 20-23, 2020; Minneapolis, MN, USA

## **Abstract**

With increased demands for coatings that have been used for screen protection for touch panel, insert molding, membrane touch switch, and the interior and exterior of automobile has emerged a new class of materials and processes. The hard-coating films which exhibit glass-like pencil hardness (9H) with modernized flexibility and excellent optical transparency have been developed by improving and optimizing the coating formulation and coating process. The coated film showed superior abrasion, scratch, chemical resistance, and anti-fingerprint properties.

Anti-reflective (AR) films can greatly improve readability under sunlight by reducing surface reflection. To produce optimized, cost-effective AR coatings, reflection simulation program of single and multi-layered thin films has been developed and utilized using the method of characteristic matrix of layered thin films and CIELAB Coordinate. The luminous reflectance (Y) reached 0.9 % when a single layer of low refractive index (RI) solution was coated on the substrate. The Y reached below 0.6 % when an optimized low RI and high RI double layers formulation was coated on clear hard coated substrate.

Kimoto adds high hardness value and multi-functionality by applying a variety of proprietary coatings to plastic substrates on one or both sides.

## **Introduction**

With increased demands for coatings that have been using for screen protection for touch panel, insert molding, membrane touch switch, and the interior and exterior of automobiles, has emerged a new class of materials and processes. Furthermore, flexible displays and flexible sensors on plastic bring transformational advantages to products including ability to modify shape, lightweight, thinness and durability while providing a path to low cost. The applications include automotive, digital signage, consumer electronics, biometrics and healthcare.

When hard-coating treatment is performed on a transparent plastic film substrate to produce a hard-coated film, thermosetting resins or ionizing radiation-curable resins such as ultraviolet (UV)-curable resins are generally used to form a thin hard-coating layer with a thickness of about 2 to 10  $\mu\text{m}$  on the transparent plastic film. If such resins are applied to a glass material, the resulting hard coating layer can exhibit a pencil hardness of 4H or more. If a hard-coating layer with a thickness of 5-10  $\mu\text{m}$  is formed on a transparent plastic film substrate, the pencil hardness of the layer can be generated 3H or less. This hardness range of 3-4H does not provide sufficient hardness for flexible displays and flexible sensors application. Various studies have been conducted to improve scratch resistance, mechanical strength of the hardened materials, adherence of a certain material with other materials it contacts, and the like, by means of blending an organic material and an inorganic material. In particular, the combination of an inorganic material and a polymerization-curing organic material, an alkoxy silane having a polymerizing group, and/or a hydrolyzed condensation product thereof, have attracted significant attention in the literature [1-8]. However, the scratch resistance and the mechanical strength of the thus obtained hardened materials are unsatisfactory, because the polyalkoxy polysiloxane and the polymerizing silane-coupling agent do not react well, and the resultant introduction rate of the polymerizing group is low. The first part of in this paper discusses how to increase hardness of cationic epoxy polymerization with polyhedral oligomeric silsesquioxane (POSS) [9-13].

With more and more electronic devices being used outdoors and in portable applications, daylight readability has become a critical factor in the display market. One way to address this issue is to increase the display's backlight luminance. This is not an ideal solution for some portable or small-size applications as it increases power consumption and results in thicker displays. Another way to solve this issue is to add a layer of antireflection coating, which improves readability in any lighting condition without increasing power consumption or bulkiness.

Both anti-glare and anti-reflective treatments represent ways to improve or optimize readability of a displayed image or clarity of displayed image [14-16]. Readability is essential for the optimum performance of any displays and the ability to process visual information clearly, quickly and comfortably (minimal eyestrain) is important. Both anti-glare and anti-reflective methods improve readability, but resolve the problem using different mechanisms to address the different causes of reduced readability. Thin film anti-reflection coatings greatly reduce the light loss in multi-element layers by making use of phase changes and the dependence of the reflectance on index of refraction. A single quarter-wavelength coating of optimum index can eliminate reflection at one wavelength. Multi-layer coatings can reduce the loss over the visible spectrum. The second part of this paper presents a computational process utilized for the numerical design and optimization of antireflection coatings and roll to roll process (R2R).

## **Materials, Experiments and Coating Process**

### **1. UV Curable Formulations**

For the high hardness hard coating, the formulation was analyzed by using different type of epoxy polymers, the cationic photo initiators, polyhedral oligomeric silsesquioxanes (POSS), silica oxide nanoparticles (20-40 nm), and additives. The UV curable formulations for AR coatings include oligomers and monomers such as urethane acrylic oligomers and monomers, amine, hydroxyl, carboxylic acid, and ethylene oxide functional (functionality 3 to 9), photo initiators, pigments and other additives. Oligomers and monomers were obtained from Sartomer, and other similar companies, and photo initiators were obtained from Ciba Chemical. Silica oxide nanoparticles were used as low RI pigments, and zirconium oxide nanoparticle were used for high RI pigment. Other pigments were obtained from EVONIK industry and Nissan Chemical (nano and micro sized silica oxide), and additives were obtained from BYK. The coated films were UV cured using F600S, 600 watt/inch from Fusion.

### **2. Computer Simulation**

The characteristic matrix method was used to simulate a reflection spectrum for multi-layered thin films. The program was coded and carried out with a Mathematica (Wolfram Research). Thicknesses and RIs of layers were used as parameters for the program. A luminous reflectance is represented by Y and calculated under the condition of D65 illuminant and 2 degrees of viewing angle. Y is one of the tristimulus values for specular reflected light. The CIE 1976 a, b chroma ( $C_{ab}^* = (a^{*2} + b^{*2})^{1/2}$ ) was calculated by using CIELAB color coordinate concept for reflected light, where  $a^*$  represents red-green chroma perception and  $b^*$  represents yellow-blue chroma perception.

### **3. The Coating Structures**

The high hardness hard coating was fabricated on a PET, PC, TAC, and PI by R2R process. A schematic of how AR coating layers are fabricated on substrate is shown in Figure 1. There was always a hard coating (HC) layer between the AR coating layers and the substrate. The HC layer can be optically clear or AG with RI of 1.51. Oligomer/monomer, dispersed silica oxide, and zirconium oxide were used to formulate low and high RI's AR layers.



Figure 1. Anti-reflective Coating Structure

### **4. Coating Process**

Kimoto has developed R2R coating methods using proprietary coating formulations. The high hardness coating and AR coatings have been fabricated on 50– 175 microns of PETs, PC, PI, and 80 microns of TAC.

The low RI, high RI, and UV hard coating layers have been fabricated on 100 class production line. Simplified process flow is shown in Figure 2.

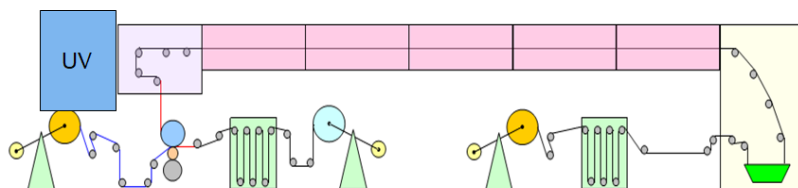


Figure 2. The Coating Process Flow

## 5. Characterization

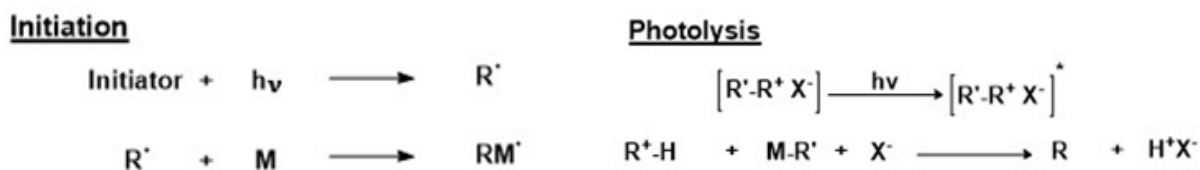
Optical properties such as haze, clarity, and transmittance were measured by BYK Haze-Gard Plus. Gloss was measured by BYK Gardner micro-TRI-gloss. Hardness was tested with ASTM D3363 method. Our adhesion test was performed using the following procedure: 1 inch of Nichiban tape was applied to the coated film surface and this tape was pulling off the coating very quickly to observe. Any damage to the coating was recorded (minimum three testing cycles). The RI of coated films was measured with M-2000U Ellipsometer (J.A Woollam) and Prism Coupler 2010 (Metricon). Reflectance and transmittance of coated films were measured by UV-Vis-NIR (Solid spec – 3700, Shimadzu). Surface of coated films was evaluated by using Scanning Probe Microscope, NanoNaviReal Probe Station (Probe: DF20P2, Hitachi High-Technologies).

## Results and Discussion

### I. Photo-polymerization System

Photo polymerization includes free radical polymerization and cationic polymerization. The difference between two polymerizations is mechanisms of photopolymerization. The free radical initiated by UV light makes photo polymerization of polymers. In cationic polymerization, strong acid space converted from cationic photo initiator when it absorbed UV radiation initiates polymerization. The mechanisms of free radical and cationic polymerization show in Table 1.

Table 1. Mechanisms of Free Radical and Cationic Polymerization  
Free radical photo polymerization                      Cationic photo polymerization



UV-curable resins that utilize a cationic photopolymerization mechanism behave differently than the free-radical polymerizable resins. While cationic resins use UV light to initiate polymerization, these systems utilize completely different photo initiators, monomeric materials and have their unique advantages and disadvantages in product and process selection, as shown in Table 2.

Table 2. Free Radical and Cationic Photo-polymerization Systems

	Free radical photo-polymerization	Cationic photo-polymerization
1	Free-radical initiate polymerization	Charged strong acid initiate reaction
2	Short life of free-radical	Long life of cationic charged space
3	High shrinkage	Low shrinkage
4	Oxygen inhibition	no Oxygen inhibition
5	Not stable at high temp	Stable at high temperature

It is important to note that for polymerization to occur, only the acid is necessary, not the light energy which produce the acid. Strong acid has two benefits over a free radical. The first benefit is the active life of the acid catalyst is much longer than a free radical. The active life of a free radical is measured in seconds while the charged active acid space can survive for days. The second benefit is that acid catalysts are not consumed in the polymerization reaction whereas free radicals are. These two differences allow cationic polymerization reactions to continue curing after UV exposure, unlike free-radical reactions.

Cationic crosslinked layers shrink less than typical free-radical systems. The mechanism behind polymerization causes shrinkage for both free-radical and cationic reactions. Unique to cationic reactions, however, is the epoxy ring opening step before molecule-to-molecule interaction. This step actually lengthens the molecule and can offset the shrinkage caused by polymerization. The ring opening step is unique to cationic epoxy and does not occur in free-radical acrylate reactions.

Free-radical UV polymerization can be terminated early by oxygen in the air. The oxygen itself will react with the free radical, stopping chain initiation and also preventing further chain extension through premature chain termination. This leaves the surface of the material unfinished and tacky. Cationic curing system is not inhibited in this fashion. This allows them to cure in ambient conditions with better ease than free-radical UVs.

Typical free-radical acrylate products will not survive temperatures above 120°C and, even if they do, the product could possibly yellow and diminish in physical properties. Cationic epoxies polymerized products, however, can survive temperatures as high as 200°C.

## II. High Hardness Film

### 1. Optical and physical property of coated materials

It is difficult to reach high hardness scratch resistance film by using free radical photopolymerization polymeric materials. The inorganic materials are normally brittle and polymer materials typically lack wear resistance. The hybrid materials which include inorganic nano particle and organic curable polymer are ideal material to create glass like wear resistance and plastic like bendability.

Hybrid Plastic Inc. has developed new hybrid molecule which has inorganic silsesquioxane at the core and organic functional group attached at the corner of the cage as shown in Figure 3 [9-12]. The well knowing fast cure photopolymerization in coating is the cationic photo-initiated epoxide polymers. We have created formulations by analyzing epoxy polymers, POSS type, cationic photo initiators, additives, and have developed coated materials by R2R process which show high hardness and moderated flexible. The coating solution was fabricated on the PET, TAC, PC, and PI by UV-curing. The UV cured layer was post cured at 80-110 °C. The optical properties, thermal stability, and mechanical properties of the fabricated films were measured and the results are shown in Table 3.

The coated films have excellent transparency of over 90%, low haze below 1%, good solvent and scratch resistance, high hardness, and good weather ability, and the optical and physical properties did not change at 60°C with 90 % humidity for 1000 hours.

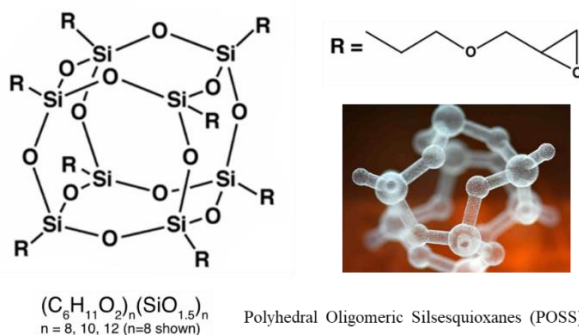


Figure 3. Representative Structures for Oxirane POSS

Table 3. Optical and Physical Properties of Coated Films

	Test method	U/M	Measured
Haze	ASTM D1003	%	≤ 1.0
Transmittance	ASTM D1003	%	≥ 90
60° Gloss	ASTM D523	%	≥ 150
Clarity	BYK Gardner	%	≥ 90
Pencil hardness	ASTM D3363	-	H - 9H
Adhesion	ASTM D3359	-	5B
Steel wool scratch resistance	KTI method	-	PASS
Chemical resistance	Ketone, Toluene, IPA, Ester, Hexane	-	PASS
Durability test for 1000 hours	60°C and 90 % humidity		No change

## 2. The hardness of the coated materials

The scratch resistance of coating on different substrates was evaluated through pencil hardness tests with a constant applied load of 4 pound according to ASTM D3363 method and the results are shown in Figure 4.

The pencil hardness was increased by increasing the coating thickness, the hardness was 9H on the PET, TAC, PI, and 7H on the PC when the thickness was increased to 50 μm. It should be noted that the coating at a thickness of 50 μm was rated with a pencil hardness of 9H, the highest hardness index, which is comparable to that of glass surface.

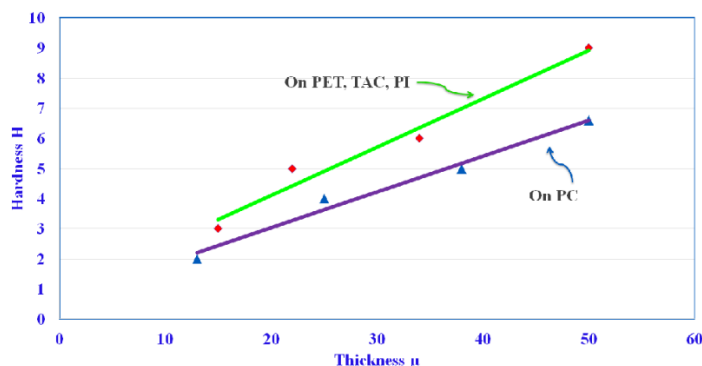


Figure 4. The hardness of coated films with thickness

## 3. Formulation, process, and hardness

Inorganic silsequioxane impact hardness and epoxy polymers give a flexibility to the coated materials. The nanosilica with 40 nm was incorporated into the formulation and its properties were investigated. Higher hardness was reached when POSS/nona-silica was blended at a ratio of 60/40. Nano-silica in combination with POSS can be viewed as two reinforcing agents combined into one and can be considered a tool toward the formulation of hard and durable coatings [10]. When the effects of ratio of inorganic and polymeric parts on the hardness of coating were analyzed, the hardness was increased when inorganic portion was increased. 9H pencil hardness was reached when inorganic portion was increased to 65%, as shown in Figure 5. The flexibility was increased when the epoxy polymer amount was increased or thickness was decreased.

Once a cationic photoinitiator absorbs UV radiation, the initiator molecule is converted into a strong charged acid species and strong acid initiates polymerization. The speed of cationic photopolymerization was higher at elevated temperature, and the polymerization reaction occurs slower at lower temperature. The reaction speed was checked at room temperature, and we found that the pencil hardness increased up to 6H hardness after 5 days.

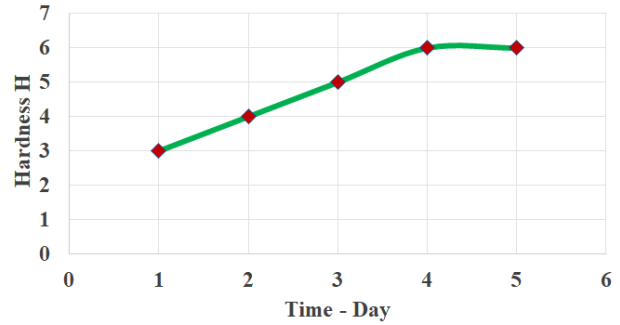
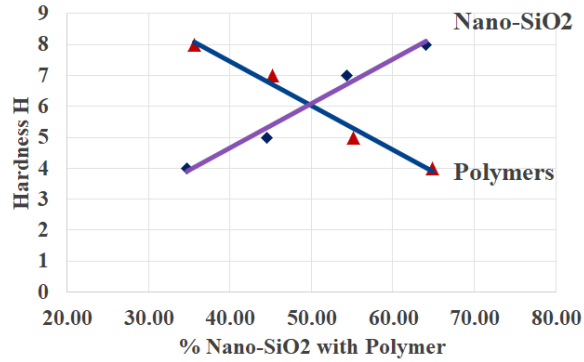


Figure 5. Effect of ratio of polymer and nano- SiO2 (left) and time (right) on hardness

The coated film was UV cured and kept at room temperature

#### 4. Cycloaliphatic epoxy and other type of epoxy

Oxetane alcohol (3-ethyl-3-hydroxymethyl oxetane), dioxetanyl ether, and xyllylene Oxetane were tested with aliphatic cyclohexane epoxy (3,4-Epoxy cyclohexylmethyl-3,4-epoxycyclohexanecarboxylate). The reaction speed increased with these oxetane, but hardness was decreased. The cycloaliphatic epoxy was the main epoxy utilized for the system to achieve high hardness film. This finding was not surprising as the aliphatic cyclohexane epoxy is well known to quickly undergo cationic polymerization. The difunctional nature of the bisoxetane is also well disposed to crosslinking as is the polyfunctional POSS. Formulations using the mono-oxetane coagent also provided increased adhesion and flexibility relative to the bis-oxetane in combination with cycloaliphatic epoxy. This finding is not surprising given the presence of a hydroxyl group on the mono-oxetane [10].

### III. Anti-Reflective Film

Because the largest change in refractive index occurs at the interface between air ( $n=1$ ) and the substrate ( $n=1.5$ ), an effective AR or AG coating of a display substrate should be present at the topmost layer, i.e., in direct contact with the air or ambient surroundings, and therefore, should be sufficiently durable to protect the device against abrasions and scratches. An AR coating is generally more sophisticated than an AG coating. An AR coating normally requires creation of a precisely controlled multilayer structure that could engage reflections from each interface to a destructive interference in the viewing direction [17-21]. Such a multi-layered AR coating must have a prescribed combination of refractive index variations as well as controlled layer thickness to achieve the desired destructive interference over an entire visible spectrum.

The AR layer is only effective when the refractive indices and thicknesses coordinate such that the destructive interferences occur among the reflections from several different interfaces and over a frequency range eliminating all reflections. However, constructing such a sophisticated and precisely layered structure is challenging, especially with regards to the processing speed and cost. We reported AFP, AG, AS, and AR structure and coating process [22-25]. In this research, computer simulation was conducted and the learnings from the simulations were used to designed experiments and fabrication conditions for single and multilayer AR films.

#### Simulation of reflection spectrum and lab results

##### 1) Single layer type AR (1LAR)

The refractive index of the clear UV hard coated (HC) layer was 1.51, same as substrates. The RI of low reflective index ( $n_L$ ) layer should be lower than 1.51. The thickness of low R.I. layer was calculated by  $550/n_L/4$ , the simulated RI of the  $n_L$  layer with the luminous reflectance Y (minimum value) is shown in Fig. 6. To achieve Y % of 1.0 or less, the refractive index of  $n_L$  layer must be between 1.14 and 1.36. We targeted this range of RI number when we created low RI layer' formulations.

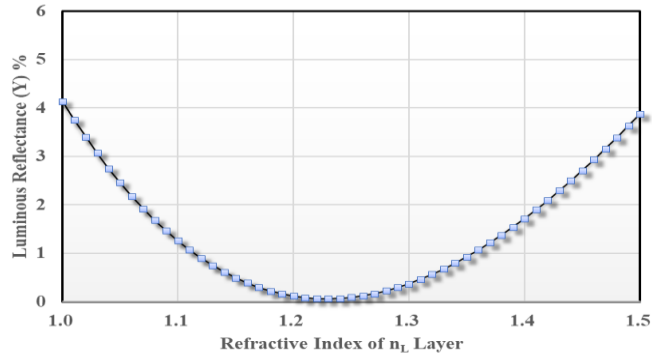


Figure 6. The simulation of refractive index of  $n_L$  layer with luminous reflectance  $Y$ .

2) AR of 1LAR

The formulation of low RI layer was created and coated on the clear UV hard coating using 50 micron of PET, and reflected spectrum is shown in Figure 7. The pattern of luminance reflectance of coated sample matched that of calculated luminous reflectance  $Y$ , which is 1.14 %.

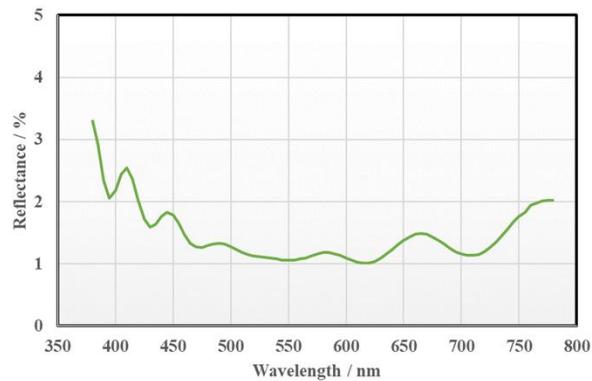


Figure 7. The observed reflection spectrum of the trial product for 1LAR.

3) A single layer AR on the AG surface

The low reflective index (TU-2360) solution was coated on the AG-HC (G90: refractive index of formulated component is 1.51) by using TAC (P980) film. KIMOTO's product name is KB-stick VIST. The measured reflection spectrum of the VIST and the calculated spectrum of 1LAR on the flat surface are shown in Figure 8. The measured and calculated luminance reflectance ( $Y$  %) matched at 550 nm with value of 0.90-0.93; but calculated  $Y$  % was higher than measured  $Y$  % on the coated sample at wavelength below 530 nm and above 630 nm. For AR on AG surface, a part of the reflected light was scattered by rough surface of AG. Since usual reflection spectrum is measured only for the specular reflection, the VIST has lower reflectance than the calculated spectrum of 1LAR on the flat surface over the visible spectrum. The target reflectivity ( $Y$ %) of 1.0 was achieved for VIST.

4) The double layers type AR (2 LAR)

The structure right side of Figure 1, low RI/high RI/HC was used to coating 2LAR. Parameter and alphabets used to calculate and simulate whole system are as follow;  $Q$  is the  $\frac{1}{4}$  wavelength thickness,  $H$  is the  $\frac{1}{2}$  wavelength thickness,  $d_H$  and  $d_L$  are the thicknesses of the  $n_H$  and the  $n_L$  layers respectively. The low and the high refractive index materials were simulated with  $n_L = 1.35$  and  $n_H = 1.70$ . These materials are selected from the viewpoint of availability.

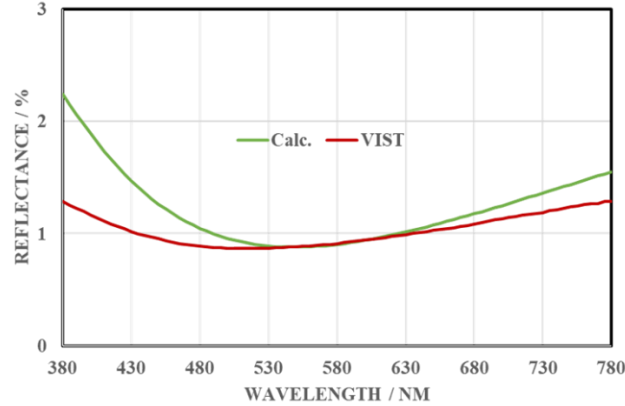


Figure 8. The measured spectrum of the VIST and the calculated spectrum of 1LAR on flat surface.

Following 2 types of designs are going to be analyzed for the double layer structure.

**QQ type of 2LAR**

The QQ type of 2LAR consists of quarter wavelength thickness of low RI's layer on the top, and a quarter wavelength thickness of high RI's layer on HC layer (Fig. 1). The simulated reflectance of QQ and HQ type of 2LAR, and 1 LAR vs. wavelength are shown in Figure 9. The luminance reflectance (Y%) of QQ type (green line) was much lower than that of 1 LAR (black line) at 550 nm, but Y% of QQ type increased below 480 nm and above 650 nm.

**HQ type of 2LAR**

The HQ type of 2LAR consists of a quarter wavelength thickness of low RI's layer on the top, and half wavelength thickness of high RI's layer on the HC layer (Fig. 1). The simulated Y % vs. wavelength is shown as red line in Figure 9. The Y % of QQ was much lower (0.1 %) than that of HQ and 1LAR at 550 nm, and the Y % of HQ and 1LAR were same at 550nm (0.93%). However, the Y % of HQ was lower (0.2 %) at 450 nm and 700 nm than 1LAR and QQ. The results show that Y % of 2LAR is lower than that of 1LAR overall, and lower regions of Y % of 2LAR compared to 1LAR depend on coating thickness. The chromaticity change was calculated using CIELAB Coordinate,  $C^*_{ab} = (a^{*2} + b^{*2})^{1/2}$ , where  $a^*$  represents red-green chroma perception and  $b^*$  represents yellow-blue chroma perception. The calculated chromaticity and reflectance Y's of the 1LAR and the 2LARs are shown in Table 4. The chroma,  $C^*_{ab}$  was increasing in the following order 1LAR < HQ < QQ, and Y % at higher wavelength range (650 nm – 800 nm) was decreasing in order of QQ > 1LAR > HQ.

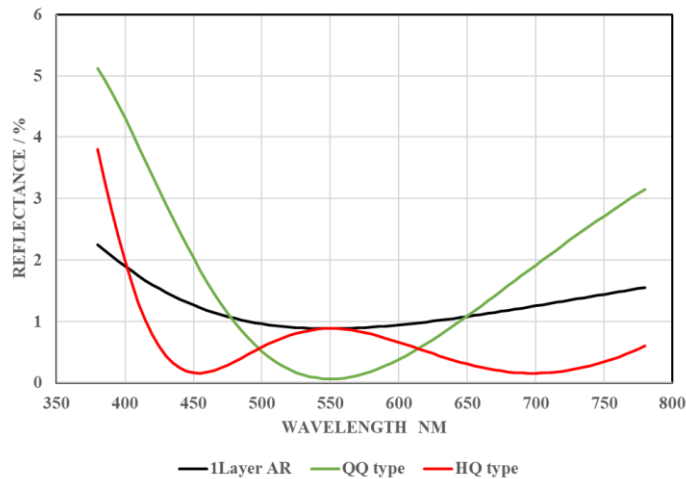


Figure 9. The simulated luminous reflectance Y of 1 LAR and 2 LAR vs. wavelength.

Table 4. The calculated CIE 1976 a, b chroma and Y of the 1LAR and 2LAR

	$d_H$ [nm]	$d_L$ [nm]	Y [%]	$a^*$	$b^*$	$C^*_{ab}$
<b>QQ type</b>	81	102	0.31	16.47	-21.06	26.7
<b>HQ type</b>	162	102	0.72	-5.10	6.18	8.0
<b>1LAR</b>	—	102	0.93	3.15	-4.39	5.4

5) The effect of thickness  $d_H$  of the high RI layer on luminance reflectance

The thickness  $d_H$  of the high RI layer on clear HC, and anti-glare HC was changed from zero to 220 nm; and influence of  $d_H$  on luminance reflectance of QQ and HQ types were checked, and the results are plotted in Figure 10, where the green line is for clear HC and yellow line for the AG-HC.

The Y % was decreasing to minimum of 0.38 when  $d_H$  was increasing to 95 nm, then Y % was increasing when  $d_H$  was continuing to increase above 95 nm on the clear HC; while Y % was decreasing to 0.60,  $d_H$  was increasing to 150 nm, then Y % was a plateau of 0.6 when  $d_H$  was continued increasing to 220 nm on the AG-HC. The only differences is surface morphology of clear HC and AG-HC and why the observed Y % values vary needs further investigation.

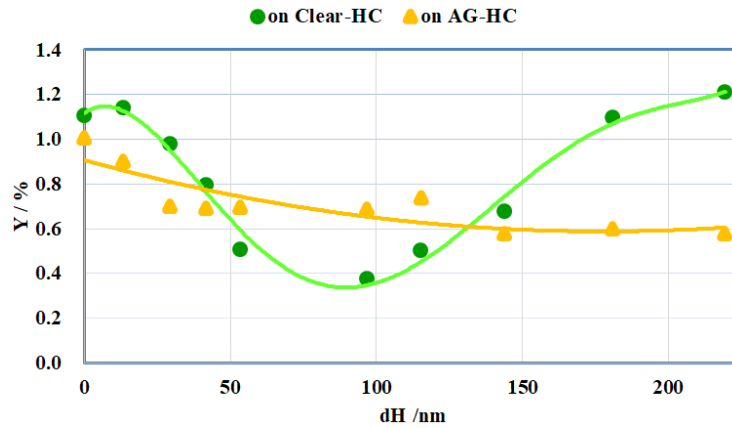


Figure 10. The luminance reflectivity with  $d_H$  on clear-HC and anti-glare-HC

**Fabricated anti-reflective film and thermoform able film**

1) Anti-reflective TAC

According to computer simulation results and optimized formulation & process parameters, anti-reflection layer was fabricated on TAC film by using KIMOTO's 100 class clean room, the results is shown in Figure 11. The KIMOTO's VIST has 1.2 % reflection and good optical & physical properties that are suitable for flat panel displays application.

2) Thermo-formable PC

The thermos-formable, lower reflective, lower cost screen protection film for curved display was fabricated by creating a specific UV hard coating formulation, adjusting coating thickness, and using high speed R2R coating process. The result is shown in Figure 12. The coated film has very good optical and physical properties.

3) Elongation of Formable Hard Coated Film

We tested elongation property using forming process: the distance was 7.1 mm, and elongated to 14 mm after formed without cracking, the elongation was 100 %, as shown in Figure 13. The coated film showed a very good elongation property.

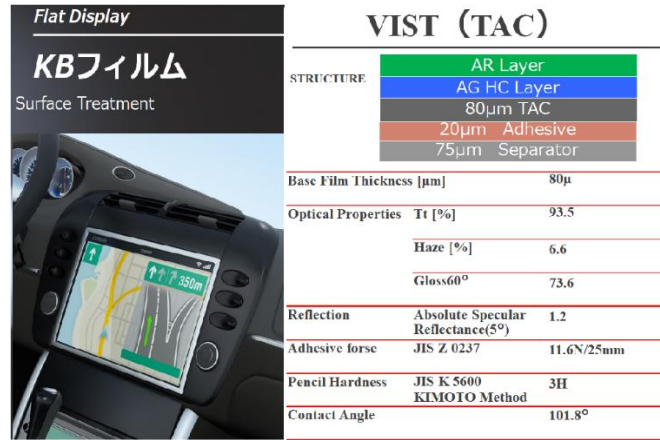


Figure 11. The VIST, anti-reflective film fabricated on TAC film

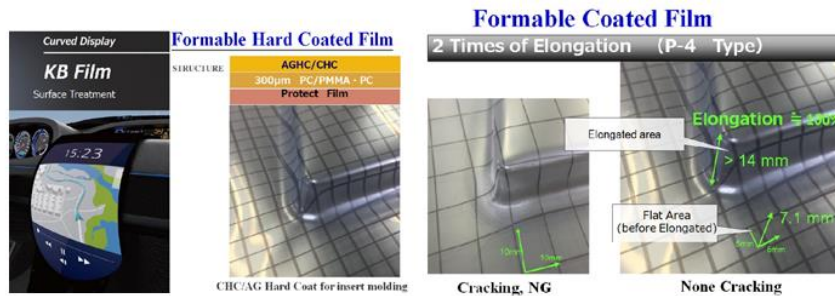


Figure 12. The thermos-formable PC film; Figure 13. The elongation property thermos-formable PC

## Conclusion

### 1. Higher hardness of coated film

9H pencil hardness, glass-like wear resistance film was fabricated on different substrates by applying and optimizing cationic polymerization formulation and coating process. The formulations which include epoxy polymers, cationic photo initiators, type of POSS, dispersed silico nano particles, and additives were analyzed in detail and we found that high hardness was created by crosslinking of epoxy polymer with epoxy of hybrid (organic-inorganic) POSS. The hardness and flexibility was a function of epoxy/Silica (POSS plus nano particle) ratio and thickness of coating layer. The pencil hardness was 9H on PET, TAC, PI, and 7H on PC when the coating thickness was increased to 50 microns and the ratio of epoxy/silica was 35/65%. This glass like wear resistance of optically clear coated film with anti-fingerprint property is an ideal screen protection film for any touch panels.

### 2. Computer simulation of reflectivity of 1LAR and 2LAR

The effect of RI, thickness, wavelength, and chromo parameters ( $C^*ab$ ) of single layer (1LAR), low RI/Clear HC/substrate, and double layer, low RI/HighRI/HC/Substrate on simulated reflectance were analyzed in detail by using Mathematica program (Wolfram Research), based on concept of characteristic matrix of layered thin films and CIELAB Coordinate. The calculated and simulated results show that (1) the RI must be 1.36 and lower in order to get  $\leq 1.0$  % reflectivity (Y); (2) the Y % of 1LAR is higher than that of 2LAR, but  $C^*ab$  of 2LAR is higher than that of 1LAR; (3) the Y % decreases in the following order 1LAR > HQ > QQ.

### 3. AR materials fabricated on the R2R coating line

The measured reflectance was 1.14 when a low RI solution was coated on clear HC using PET, and the reflectance reached 1.0 % when a low RI solution was coated on AG-HC using TAC, and these patterns of Y % vs. wavelength matched that of simulated results, showing the accuracy of the simulation method. The reflectance reached below 0.6 % when a low RI/high RI solution was coated on clear HC or AG-HC at 550 nm.

The coating thickness and conditions were controlled very well in the lab and on the production line, and results from thin coated films matched that of simulated results. We found a correlation between coating parameters and luminance refraction. Kimoto's anti-reflective film, VIST has a low reflection (1.2%), and good physical properties, and is suited for flat panel display's application. The thermos-formable PC films have 100 % elongation property and are suited for curved screen and insert molding's applications. Kimoto coated films can provide glass-like hardness and various multi-functionality by applying a variety of proprietary coatings to plastic substrates.

## References

- [1] N. Jappar; RadTech UV/EB Technology Conference, May 7-9, 2018 in Hyatt Regency Chicago, Chicago, Illinois – United States of America, “Development of Multi-functional film and R2R process”
- [2] N. Jappar; 2018 Flexible & printed electronic conference, Jan. 29 – Feb. 1, 2018; Phoenix Arizona, USA; “Multi-Functional Film and R2R Coating Process”
- [4] N. Jappar; AIMCAL USA Web Handling Conference 2018, Phoenix, Arizona, October 28 - 31, 2018; “Development of conductive film, R2R coating process”
- [5] N. Jappar; 2019 Flex Tech conference, Feb. 18-21, Monterey California, USA; “Multi-Functional Films for Displays Application”
- [6] N. Jappar; Electronic displays Conference 2019, February 27-28, 2019; Nuremberg, Germany “Functional Films for Display Application”
- [7] N. Jappar; LOPEC 2019 Shows and Conference; March 19-21, 2019, Munich, Germany; “Multi-functional films for displays application”
- [8] N. Jappar; 2020 Flex Tech conference, Feb. 18-21, San Jose California, USA; “Advanced Multi-Functional Films for Displays Application”
- [9] Joseph D. Lichtenhan; Hybrid plastic, inc., Radtech UV.EB May 7-9,2018, Chicago, IL; “POSS coating additives: Epoxy and acrylic tool kits”
- [10] Joseph D. Lichtenhan; Hybrid plastic, inc., Radtech Mach9, 2020, Orlando, FL; “POSS Oxirane and Oxetane Additives for energy cure coating and adhesives”
- [11] Joe Lichtenhan JD (2019) POSS Additives in Energy Cure Coatings: A Technical Review. Curr Trends Nanotechnol 1: 101. DOI: 10.29011/CTNT-101.100001
- [12] Marco Sangermano, etc., Pure Appl. Chem., Vol. 84, No. 10, pp. 2089–2101, 2012; “Advances in cationic photopolymerization”
- [13] Joseph D. Lichtenhan; Hybrid plastic, inc., DOI: 10.1063/1.2208355; “The mechanical properties of crystalline cyclopentyl polyhedral oligomeric silsesquioxane”
- [14] Hiroko Suzuki, etc., antiglare film and displays image, US 2004/0240070 A1
- [15] James A. Ferwerda, etc., Perception of anti-sparkle in anti-glare display screen, Journal of the SID, 2014
- [16] Tien-Hon Chiang, etc., Functional enhancing optical film, US 2008/0095997 A1
- [17] Mohtashim Saif, etc., Anti-reflective composite, US 6,266,193 B1
- [18] Arthur J. Yang, etc., Antiglare and antireflection coating of surface active nanoparticles, US 2006/0074172 A1
- [19] Yingying Sun, etc., A simple method to control the microstructure and properties of sol-gel silica antireflective coatings, RSC Adv., 2017,7, 31950
- [20] Tetsuya Asakura, etc., An anti-glare and anti-reflection film, polarizing plate using An anti-glare and anti-reflection film, and liquid crystal displays devise using the polarized plate, US 2006/0153979 A1
- [21] Daisuke Hamamoto, etc., antiglare hard coated film, US 2009/0086326A1
- [22] N. Jappar, Functional conductive film for flexible electronics and R2R coating process, Printed Electronics EUROPE 2015; Berlin, Germany; April 28-29, 2015
- [23] N. Jappar, Hybrid conductive film for flexible displays and R2R coating process, The 2014<sup>th</sup> International Meeting on Information Display; EXCO, Daegu, Korea; August 26-29, 2014
- [24] N. Jappar, Develop Functional Films and R2R Process, **RadTech 2018**, the **UV+EB Technology Conference** and Expo, May 7-9, **2018** in Chicago, IL, USA
- [25] N. Jappar, Functional Films for Displays Application, Display Week 2018, May 20-24, 2018, Los Angeles Convention Center, CA, USA